J|A|C|S
ARTICLES
Published on Web 11/01/2006

Base Pair Recognition of the Stereochemically α-Substituted γ-Turn of Pyrrole/Imidazole Hairpin Polyamides

Wen Zhang, Masafumi Minoshima, and Hiroshi Sugiyama*

Contribution from the Department of Chemistry, Graduate School of Science, Kyoto University, Sakyo-ku, Kyoto 606-8502, Japan

Received June 21, 2006; E-mail: hs@kuchem.kyoto-u.ac.jp

Abstract: Recognition of the sequences 5′-**N**GCACA-3′ (**N** = T, A, C, G) by pyrrole/imidazole polyamides with (*R*/*S*)-α-hydroxyl/α-amino-substituted γ-aminobutyric acid as a γ-turn was investigated. Four novel polyamides, **2**, **3**, **4**, and **5**, including (*R*)-α-hydroxyl-γ-aminobutyric acid (γRO), (*S*)-α-hydroxyl-γ-aminobutyric acid (γSO), (*R*)-α,γ-diaminobutyric acid (γRN), and (*S*)-α,γ-diaminobutyric acid (γSN) residues, respectively, were synthesized, and their binding affinity to T•A, A•T, G•C, and C•G base pairs at turn position was studied by the surface plasmon resonance (SPR) technique. SPR data revealed that polyamide **3**, AcImβImPy-γSO-ImPyβPy-β-Dp, with a γSO turn, possesses a marked binding preference for T•A over A•T with a 25-fold increase in specificity, despite low binding affinity relative to **2**, with a γRO turn. Similarly, AcImβImPy-γSN-ImPyβPy-β-Dp (**5**), with a γSN-turn, gives rise to a 8.7-fold increase in specificity for T•A over A•T. Computer-assisted molecular modeling suggests that **3** binds more deeply in the minor groove of the T•A base pair relative to the A•T base pair, allowing hydrogen bonding to O2 of the thymine at the turn position, which explains the SPR results. These results suggest that γSO and γSN may function as T-recognition units at the turn position, as well as a γ-turn in the discrimination of polyamides.

Introduction

N-Methylpyrrole (Py)-*N*-methylimidazole (Im) polyamides can recognize predetermined DNA sequences in the minor groove of B-DNA.[1,2] All four Watson−Crick base pairs can be recognized using different pairings of three aromatic amino acids, that is, with a pairing of Im/Py or Py/Im specifying G•C or C•G, respectively, and a Py/Py pairing being able to degenerately recognize A•T or T•A base pairs (Figure 1).[3] A hydroxypyrrole (Hp) and Py pair (Hp/Py) distinguishes T•A from A•T base pairs;[4] however, there are disadvantages in using Hp, such as: (1) the Hp residue can degrade in solution over time in the presence of acid or free radicals, (2) it has a lower affinity for T bases relative to Py, and (3) Hp at the N-terminus of polyamides has almost no specificity for any base of the Watson−Crick base pairs.[5]

Because polyamides composed of more than five continuous Py's or Im's are too curved to fully match the curvature and twist of the DNA helix, their binding specificity decreases.[6,7] To solve the problem, the Dervan group introduced β/β pair into the construction of Py/Im polyamide, in which it serves as a "spring" to adjust the crescent-shaped polyamides so that they are able to match the curvature and twist of B-DNA and act as T/A readers.[8] Such aliphatic modification and displacement of the central monomers in polyamides have been shown to greatly affect their DNA binding affinity and sequence recognition selectivity.[9,10] In a previous study using the surface plasmon resonance (SPR) technique, we investigated the influence of the introduction of stereochemically α-hydroxyl/α-amino-modified γ-aminobutyric acid on the recognition of DNA base pairs by hairpin polyamides in the minor groove.[11] We found that (*S*)-α-hydroxyl-γ-aminobutyric acid can specify for 5′-TG-3′ by forming specific hydrogen bonds.

These encouraging results motivated our interest in the exploration of the ability of stereochemically α-hydroxy/α-amino-modified γ-aminobutyric acids as a γ-turn in hairpin polyamides to discriminate DNA bases at the turn position in the minor groove. Surprisingly, to our knowledge, there have

(1) (a) Dervan, P. B. *Bioorg. Med. Chem.* **2001**, *9*, 2215−2235. (b) Bando, T.; Sugiyama, H. *Acc. Chem. Res.*, published online August 22, 2006, 10.1021/ar030287f.
(2) Dervan, P. B.; Edelson, B. S. *Curr. Opin. Struct. Biol.* **1999**, *13*, 284−299.
(3) (a) Pelton, J. G.; Wemmer, D. E. *Proc. Natl. Acad. Sci. U.S.A.* **1989**, *86*, 5723−5727. (b) Wade, W. S.; Mrksich, M.; Dervan, P. B. *J. Am. Chem. Soc.* **1992**, *114*, 8783−8794. (c) White, S.; Szewczyk, J. W.; Turner, J. M.; Baird, E. E.; Dervan, P. B. *Nature* **1998**, *391*, 468−471.
(4) (a) Pelton, J. G.; Wemmer, D. E. *Proc. Natl. Acad. Sci. U.S.A.* **1989**, *86*, 5723−5727. (b) Wade, W. S.; Mrksich, M.; Dervan, P. B. *J. Am. Chem. Soc.* **1992**, *114*, 8783−8794. (c) White, S.; Szewczyk, J. W.; Turner, J. M.; Baird, E. E.; Dervan, P. B. *Nature* **1998**, *391*, 468−471.
(5) (a) Marques, M. A.; Doss, R. M.; Urbach, A. R.; Dervan, P. B. *Helv. Chim. Acta.* **2002**, *85*, 4485−4517. (b) Walker, W. L.; Kopka, M. L.; Goodsell, D. S. *Biopolymers* **1997**, *44*, 323−334.
(6) Kielkopf, C. L.; Baird, E. E.; Dervan, P. B.; Rees, D. C. *Nat. Struct. Biol.* **1998**, *5*, 104−109.
(7) Kelly, J. J.; Baird, E. E.; Dervan, P. B. *Proc. Natl. Acad. Sci. U.S.A.* **1996**, *93*, 6981−6985.
(8) (a) Lamamie de Clairac, R. P.; Geierstanger, B. H.; Mrksich, M.; Dervan, P. B.; Wemmer, D. E. *J. Am. Chem. Soc.* **1997**, *119*, 7909−7916. (b) Herman, D. M.; Baird, E. E.; Dervan, P. B. *J. Am. Chem. Soc.* **1998**, *120*, 1382−1391.
(9) Trauger, J. W.; Baird, E. E.; Mrksich, M.; Dervan, P. B. *J. Am. Chem. Soc.* **1996**, *118*, 6160−6166.
(10) Floreancig, P. E.; Swalley, S. E.; Trauger, J. W.; Dervan, P. B. *J. Am. Chem. Soc.* **2000**, *122*, 6342−6350.
(11) Zhang, W.; Bando, T.; Sugiyama, H. *J. Am. Chem. Soc.* **2006**, *128*, 8766−8776.

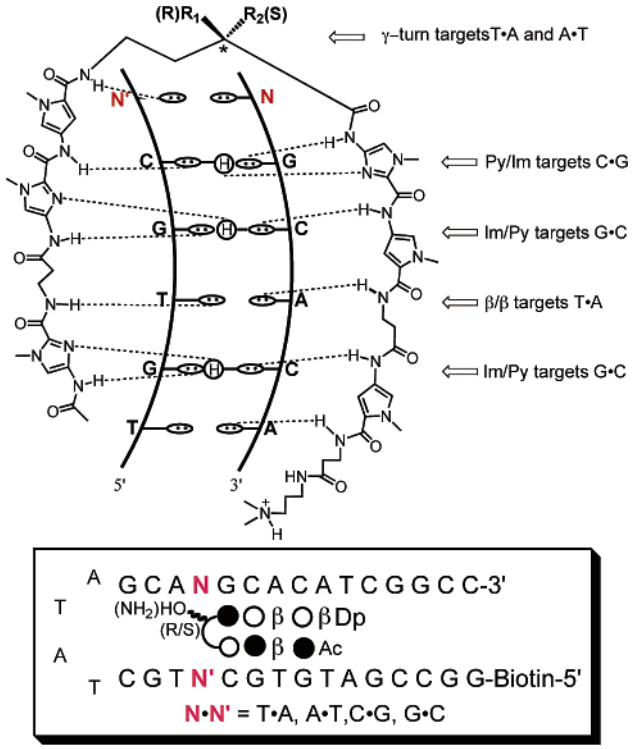

Figure 1. Schematic presentation of molecular recognition of polyamides to sequence-specific DNAs in the minor groove. Ellipses with dots represent lone pairs of the N3 of purines and the O2 of pyrimidines. Hydrogen bonds are shown as dotted lines. Circles containing an H represent the N2 hydrogen of guanine. A ball model for the polyamide/DNA complexes is given in the box at the bottom. Imidazole residues (Im) are shown as black circles, pyrrole residues (Py) as open circles, β represents β-alanine residues, Dp represents dimethylamino-propylamide, $\subset$ represents a γ-aminobutanoic acid turn residue connecting the two subunits, and Ac is acetyl.

been no reports on the ability of α-substituted γ-turns in polyamide to allow discrimination between the four Watson−Crick base pairs, T•A, A•T, C•G, and G•C, at the turn position in the DNA minor groove.

As the environment around each prochiral hydrogen at the α-position in the γ-turn of the hairpin polyamide is quite different, with the *pro-R* hydrogens sequentially pointing out of the DNA and to the wall of the minor groove, and the *pro-S* hydrogens pointing to the floor of the minor groove,[8] discrimination between DNAs by polyamides should be influenced by the nature, the size, and the stereochemistry of the α-substituent in the γ-turn at the γ-turn position after substitution of the prochiral hydrogen with a hydroxyl or amino group. The α-substituted γ-turns differ from unmodified γ-turns not only in size but also in nature, hydrogen-bonding ability, and polarity, possibly resulting in alteration of base recognition properties. Herein, we synthesized four polyamides with a stereochemically α-hydroxyl or α-amino-modified γ-turn, with γ-aminobutyric acid (**1**) as a reference. (*R*)-α-Hydroxy-γ-aminobutyric acid (γRO, **2**), (*S*)-α-hydroxy-γ-aminobutyric acid (γSO, **3**), (*R*)-α,γ-diaminobutyric acid (γRN, **4**), and (*S*)-α,γ-diaminobutyric acid (γSN, **5**) were used as the respective "turns" connecting the two subunits of the polyamide sequences in the construction of hairpin polyamides **2**−**5** (Figure 2), and their binding specificity for the four Watson−Crick base pairs was examined (Figure 1).

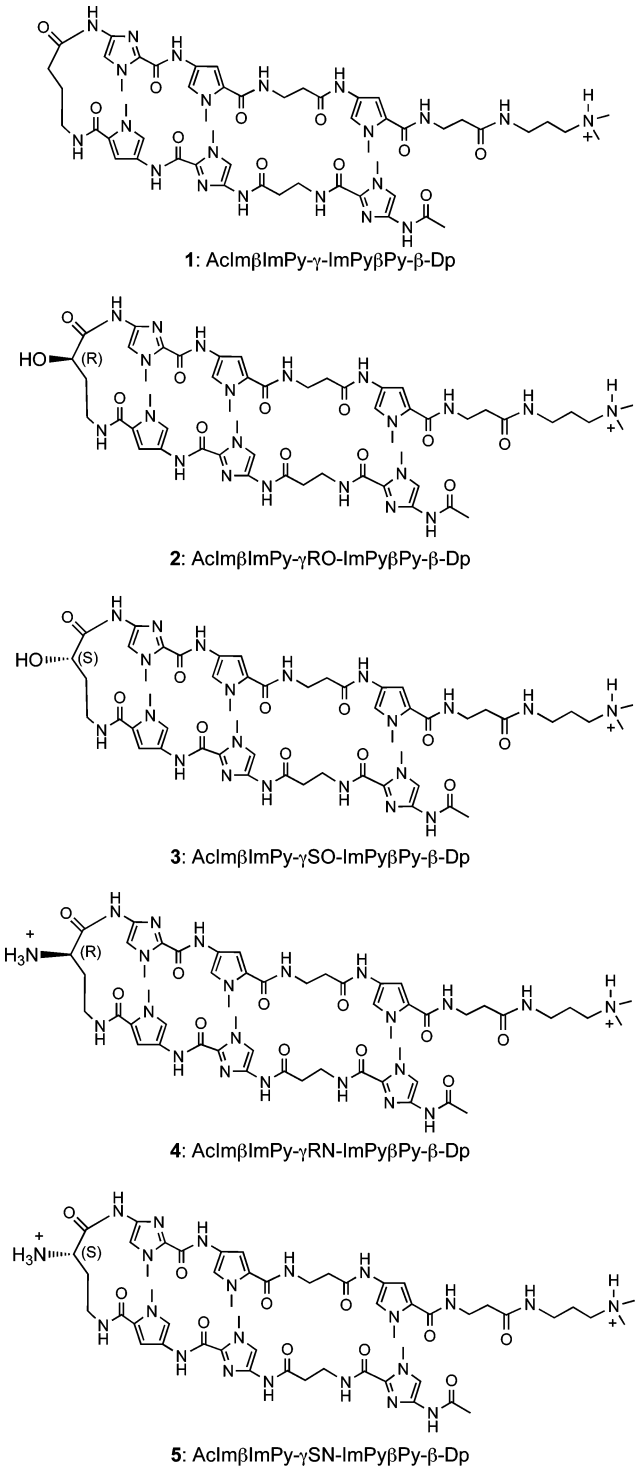

Figure 2. Chemical structures of polyamides **1**−**5** used in this study.

Results and Discussion

Synthesis. The protected optically active enantiomers **10** (*R*) and **11** (*S*) were synthesized from (*R*)-(+)-4-amino-2-hydroxybutyric acid and (*S*)-(−)-4-amino-2-hydroxybutyric acid, respectively, using our previously described methods, with almost no racemization observed under our experimental conditions.[11] On the basis of the ^{1}H NMR analysis of (*S*)-(−)-1-(1-naphthyl)-ethyl amide derivatives of **10** and **11**, we found their enantiomeric purity to be more than 97%.

Scheme 1. Polyamide Solid-Phase Synthesis Starting from Clear Resin **6**[a]

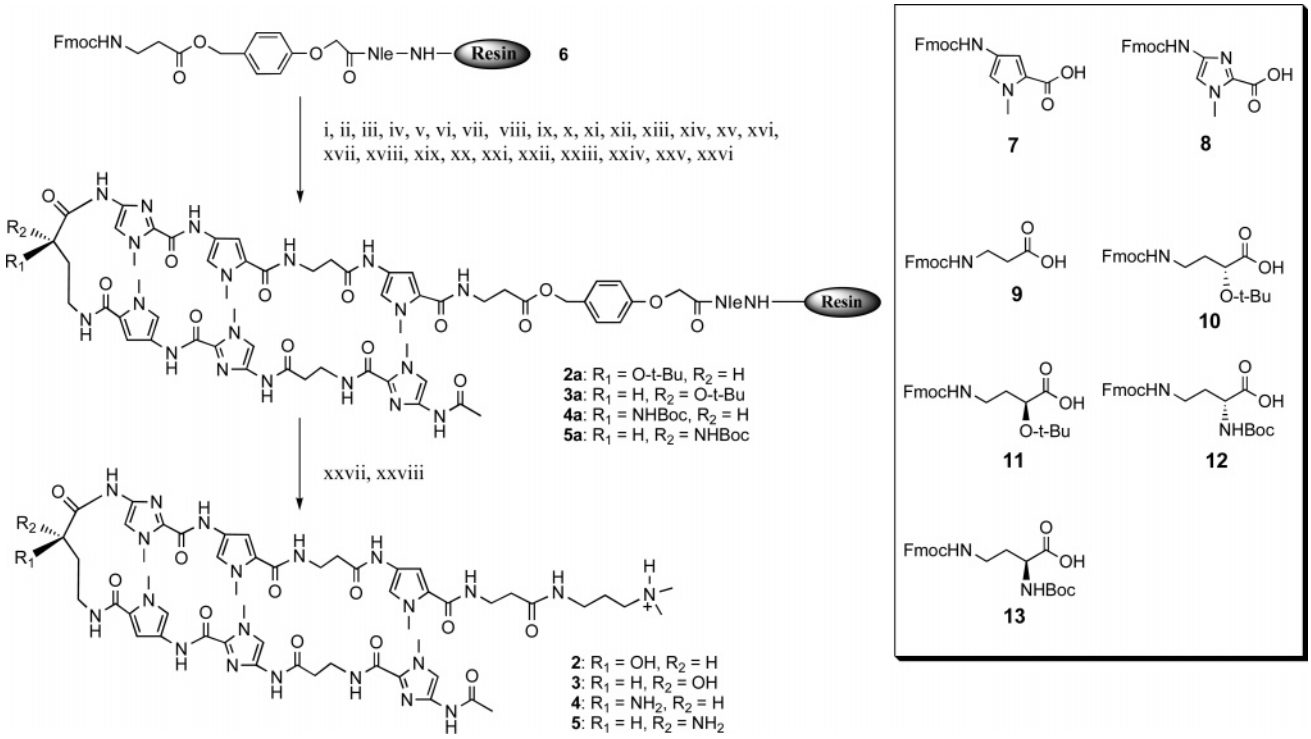

[a] Reaction conditions: (i) 20% piperidine/DMF; (ii) FmocPyCOOH, HATU, DIEA; (iii) 5% acetic anhydride + 5% pyridine/DMF; (iv) 20% piperidine/DMF; (v) Fmoc-β-Ala-OH, HATU, DIEA; (vi) 5% acetic anhydride + 5% pyridine/DMF; (vii) 20% piperidine/DMF; (viii) FmocPyCOOH, HATU, DIEA; (ix) 5% acetic anhydride + 5% pyridine/DMF; (x) 20% piperidine/DMF; (xi) FmocImCOOH, HATU, DIEA; (xii) 5% acetic anhydride + 5% pyridine/DMF; (xiii) 20% piperidine/DMF; (xiv) **10** for **2a**, HATU, DIEA; **11** for **3a**, HATU, DIEA; **12** for **4a**, HATU, DIEA; **13** for **5a**, HATU, DIEA; (xv) 5% acetic anhydride + 5% pyridine/DMF; (xvi) 20% piperidine/DMF; (xvii) FmocPyCOOH, HATU, DIEA; (xviii) 5% acetic anhydride + 5% pyridine/DMF; (xix) 20% piperidine/DMF; (xvii) FmocImCOOH, HATU, DIEA; (xx) 5% acetic anhydride + 5% pyridine/DMF; (xxi) 20% piperidine/DMF; (xxii) Fmoc-β-Ala-OH, HATU, DIEA; (xxiii) 5% acetic anhydride + 5% pyridine/DMF; (xxiv) 20% piperidine/DMF; (xxv) FmocImCOOH, HATU, DIEA; (xxvi) 5% acetic anhydride + 5% pyridine/DMF; (xxvii) *N*,*N*-dimethylaminopropylamine for *t*-butyl- and Boc-protected **2**−**5**, 55 °C, overnight; (xxviii) (a) TFA/TMS/TIS/H_2O (91/3/3/3, v/v); (b) 5 M HCl for **2**−**5**.

Polyamides **1**−**5** in Figure 2 were synthesized by a Fmoc chemistry solid-phase synthesis method starting with Fmoc-β-Ala-clear acid resin using the monomers shown in Scheme 1, on the basis of our established protocols[11] and the studies of Wurtz et al.[12] In brief, in the synthesis of polyamides, DMF was used as the solvent and HATU as the activator, and capping was employed in each cycle after coupling. After the Fmoc-Py acid **7** was activated by HATU in the presence of DIEA, the first pyrrole monomer was readily coupled to swollen resin **6** in the column of the synthesizer for 60 min, followed by coupling of the remaining aromatic residues **7** and **8**. Coupling of modified and unmodified aliphatic monomers **9**−**13** was accomplished with HATU, using the same conditions as those for coupling aromatic monomers. After the completion of the machine-assisted solid-phase synthesis, the polyamides were cleaved from resins **2a**−**5a** by aminolysis with 3-(dimethylamino)propylamine (Dp) to afford *t*-butyl-protected **2** and **3** and Boc-protected **4** and **5**. The deprotection of protected **2**−**5** was readily achieved using an optimal deprotecting agent, TFA/TMS/TIS/H_2O (91/3/3/3, v/v) to give final products **2**−**5** without racemization.[13] Likewise, polyamide **1** was also prepared using the above method. Purification of products was performed by HPLC, with overall yields ranging from approximately 10 to 20%. The structures of polyamides **1**−**5** were identified by ^{1}H NMR and ESI mass.

SPR Assay. To investigate the recognition ability of the α-substituted γ-turns for the four normal base pairs, T·A, A·T, G·C, and C·G, the SPR technique was used, with all measurements made using a Biacore X instrument using a sensor chip SA in HBS-EP buffer (0.01 M HEPES, pH 7.4, 0.15 M NaCl, 3 mM EDTA, 0.005% surfactant P20) with 0.1% DMSO (v/v) at 25 °C and based on a molecular recognition model of the polyamides to the hairpin DNAs as shown in the box at the bottom of Figure 1. The kinetic binding parameters K_A (association equilibrium constant), K_D (dissociation equilibrium constant), k_a (association rate constant), and k_d (dissociation rate constant) of the polyamides AcImβImPy-γ-ImPyβPy-β-Dp (**1**), AcImβImPy-γRO-ImPyβPy-β-Dp (**2**), AcImβImPy-γSO-ImPyβPy-β-Dp (**3**), AcImβImPy-γRN-ImPyβPy-β-Dp (**4**), and AcImβImPy-γSN-ImPyβPy-β-Dp (**5**) were determined to hairpin DNAs. Self-complementary biotinylated oligonucleotides 5′-biotin-GGCCGATGTGC**N**′TGCTATAGCA**N**GCA-CATCGGCC-3′ (34 bases, **N**·**N**′: T·A, A·T, G·C, C·G) which form double-stranded hairpin DNAs including the examined target binding sites bound by the new synthetic polyamides were noncovalently bound to streptavidin-functionalized Biacore sensor chips and binding parameters were obtained by fitting the resulting sensorgrams to a theoretical model according to

(12) Wurtz, N. R.; Turner, J. M.; Baird, E. E.; Dervan, P. B. *Org. Lett.* **2001**, *3*, 1201−1203.
(13) Beyerman, H. C.; Bontekoe, J. S. *Recl. Trav. Chim. Pays-Bas* **1962**, *81*, 691−697.

Table 1. Binding Kinetic Constants (K_D, k_a, k_d, k_t) Derived from SPR

Polyamide	K_D (10^{-7} M) k_a (10^5 $M^{-1}s^{-1}$) k_d (10^{-2} s^{-1}) k_t (10^7 RU/Ms) T·A	A·T	C·G	G·C	Specificity[a]
 **1**	0.26 (0.03)	0.22 (0.02)	31 (3)	1.5 (0.1)	0.85
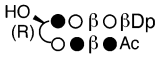 **2**	0.031 (0.002)	0.14 (0.02)	8.6 (0.8)	1.2 (0.1)	4.5
 **3**	1.1 (0.1) 3.6 (0.2) 4.0 (0.3) 20 (1)	28 (2) 1.3 (0.1) 36 (2) 9.0 (0.3)	160 (14)	340 (32)	25
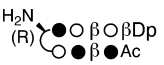 **4**	0.016 (0.002)	0.051 (0.007)	3.8 (0.4)	0.59 (0.06)	3.2
 **5**	3.9 (0.4) 0.7 (0.03) 2.7 (0.2) 5.2 (0.1)	34 (3) 0.4 (0.02) 14 (1) 3.6 (0.1)	180 (20)	720 (46)	8.7

[a] The binding specificity is given as K_D (A·T)/K_D (T·A), indicating the difference of binding between A·T and T·A. Data of the mass transfer rate constant, k_t, for the binding of polyamides **3** and **5** to T·A and A·T, respectively, suggest that mass transfer has very little influence on k_a and k_d under our experimental conditions. The number in parentheses represents the standard error.

previous studies.[11,14−16] Their binding properties, including affinity, specificity, and stoichiometry, were also evaluated through equilibrium and kinetic analyses (Figure 3, Table 1, and Supporting Information Figure S1).

Effects on Binding of the Stereochemistry of the Hydroxy Substituent in the γ-Turn. The results of the SPR studies are summarized in Table 1. Polyamide **1**, with a γ-turn (**1**), showed preferential binding to T·A and A·T base pairs relative to C·G and G·C base pairs. However, it could not discriminate T·A and A·T base pairs; the T-specificity, which is the binding to the sequence 5′-**T**GCACA-3′ over the binding to the sequence 5′-**A**GCACA-3′, was 0.85. Importantly, the introduction of amino and hydroxy groups to the γ-turn dramatically changed the binding affinity of the Py/Im hairpin polyamides. The results are consistent with the previous observation that the α-prochiral hydrogen in the γ-turn is in proximity to the suger C1′H of the nucleotide at the γ-turn.[8a] It was found that γRO-turn linked hairpin polyamide **2** had about a 10-fold increase in the binding affinity to T·A base pairs relative to **1**; the T-specificity was 4.5. The former is possibly caused by the fact that the α-hydroxyl group in the *R*-configuration is directed away from the floor of the DNA minor groove, with a resultant favorable electrostatic effect[17] without any steric clash with the DNA minor groove, thereby inducing enhancement of the binding affinity to the four base pairs, and the latter is probably partially ascribable to differential steric interactions of the α-position in the *R*-hydroxy-modified γ-turn with any base at the turn position, leading to a 4.5-fold increase in specificity for discrimination of T·A over A·T (Table 1 and Supporting Information Figures S1A and S1B).

In contrast, the γSO-turn linked hairpin polyamide **3** was found to bind weakly to the four base pairs T·A, A·T, C·G, and G·C relative to **2**, but polyamide **3** favorably binds to the sequence with the T·A base pair with a 25-fold increase in specificity, indicating that the *S*-hydroxyl group is specific for T bases at the turn position. The weak binding with higher specificity to T·A base pairs is possibly due to the balance of two factors: the *S*-hydroxyl substituent pointing toward the floor of the DNA minor groove to form a hydrogen bond with the O2 of the T base at the turn position, and a steric clash with the bases.[8a,18] It is noteworthy that the binding affinity to A·T and G·C of **3** with γSO-turn is significantly decreased by 199- and 282-fold, respectively, compared to that of **2** with a γRO-turn, implying that there exists a significantly larger steric clash at the γ-turn between the α-hydroxyl group and the C_2H of the A and the NH_2 of the G, respectively.

To quantitatively distinguish the binding properties of these polyamides, we evaluated the free energy change ($\Delta G°$, kcal/mol) from the dissociation equilibrium constant (K_D) upon the formation of the polyamide/DNA complex (Supporting Information Table 1). The binding of **2** to the T·A base pair is 1.9-fold more energetically favorable than the binding to the A·T base pair. The improved binding stability to the T·A base pair may be explained through the molecular interaction kinetics obtained from the SPR assays. As shown in Figure 3A,B and Table 1, after **3** associates rapidly with the T·A base pair to reach a steady state at the low concentration of 50 nM, it dissociates 9-fold more slowly from the **3**-5′-**T**GCACA-3′ complex than from the **3**-5′-**A**GCACA-3′ complex, which reflects different molecular interactions in both recognition events. This observation suggests the possibility that there is a relatively strong interaction, such as a hydrogen bond, between the *S*-OH and the O2 of the T at the turn position to dominate the discrimination kinetics for T·A. This possibility is further

(14) Davis, T. M.; Wilson, W. D. *Anal. Biochem.* **2000**, *284*, 348−353.
(15) Tanious, F. A.; Hamelberg, D.; Bailly, C.; Czarny, A.; Boykin, D. W.; Wilson, W. D. *J. Am. Chem. Soc.* **2004**, *126*, 143−153.
(16) Biacore AB. In *BIAapplications Handbook*; Biacore AB: Uppsala, Sweden, 1998; p 3-2.
(17) (a) White, S.; Baird, E. E.; Dervan, P. B. *Chem. Biol.* **1997**, *4*, 569−578. (b) Swalley, S. E.; Baird, E. E.; Dervan, P. B. *J. Am. Chem. Soc.* **1999**, *121*, 1113−1120.
(18) Woods, C. R.; Ishii, T.; Wu, B.; Bair, K. W.; Boger, D. L. *J. Am. Chem. Soc.* **2002**, *124*, 2148−2152.

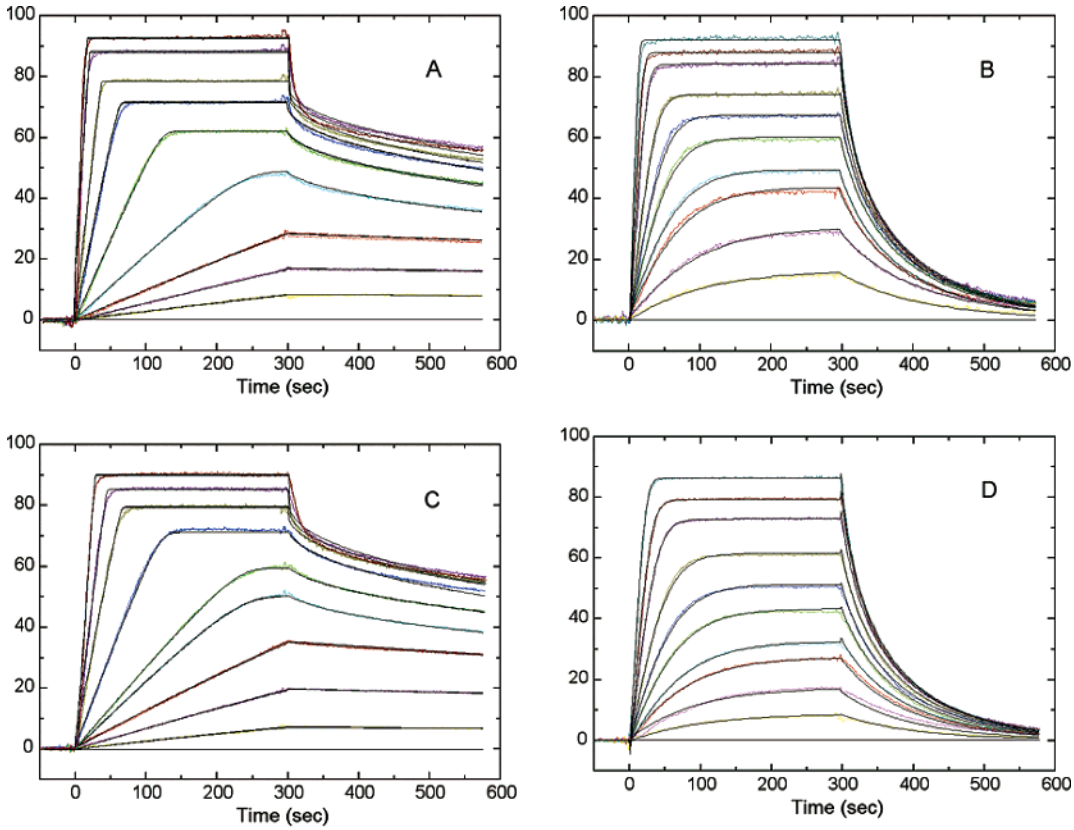

Figure 3. Typical SPR sensorgrams for the interaction of polyamides with an α-substituted γ-turn with hairpin DNAs immobilized on the surface of a sensor chip SA. The binding response is changed with time. Injection of sample solution at each concentration was repeated at least twice for binding to T•A, and the data are globally fitted to a 1:1 interaction model with mass transport. Experimental curves are shown in color and fitting curves in black. The association phase was allowed to run for 300 s to reach steady state and the dissociation phase for 280 s for all concentrations used. All experiments were done using sensor chips with almost identical DNA immobilization levels in HBS-EP buffer (0.01 M HEPES, pH 7.4, 0.15 M NaCl, 3 mM EDTA, 0.005% surfactant P20) with 0.1% DMSO (v/v) at 25 °C. (1) Polyamide **3** with an $^{S}\gamma_{\alpha-OH}$-turn for the recognition of the sequences 5′-**T**GCACA-3′ (A) and 5′-**A**GCACA-3′ (B) at concentrations of 0 (blue, lowest curve), 3.12 (light yellow), 6.25 (light magenta), 12.5 (light red), 25.0 (light cyan), 50 (light green), 100 (light blue), 200 (yellow), 400 (magenta), and 800 nM (red, highest curve), and 0 (blue, lowest curve), 3.12 (light yellow), 6.25 (light magenta), 12.5 (light red), 25.0 (light cyan), 50 (light green), 100 (light blue), 200 (yellow), 400 (magenta), 800 (red, highest curve), and 1600 nM (cyan, highest curve), respectively. (2) Polyamide **5** with an $^{S}\gamma_{\alpha-NH2}$-turn for the recognition of the sequences 5′-**T**GCACA-3′ (C) and 5′-**A**GCACA-3′ (D) at concentrations of 0 (blue, lowest curve), 3.12 (light yellow), 6.25 (light magenta), 12.5 (light red), 25.0 (light cyan), 50 (light green), 100 (light blue), 200 (yellow), 400 (magenta), and 800 nM (red, highest curve), and 0 (blue, lowest curve), 3.12 (light yellow), 6.25 (light magenta), 12.5 (light red), 25.0 (light cyan), 50 (light green), 100 (light blue), 200 (yellow), 400 (magenta), 800 (red, highest curve), and 1600 nM (cyan, highest curve), respectively.

verified in the molecular modeling studies to be described later. As expected, all SPR sensorgram results had a better global fit to a model with a mass transfer effect, suggesting a 1:1 polyamide to DNA stoichiometry for the polyamide/DNA complex. No 2:1 binding mode of polyamide to hairpin DNA was found despite the high concentrations used.

Effects of Amino Substituents on Binding. As shown in Table 1, polyamide **4**, with a γRN-turn, has much more favorable binding to all four base pairs than polyamides **1**, **2**, **3**, and **5**, displaying a 3.2-fold increase in preference for the T•A base pair over the A•T base pair (Supporting Information Figures S1C and S1D). This difference in affinity among polyamides for binding to the same sequence may result from the fact that as the *R*-amino substituent in polyamide **4** is directed at the deoxyribose wall of DNA and is proximal to the sugar/phosphate backbone of DNA, an electrostatic interaction occurring between the positively charged amino group and the negatively charged sugar/phosphate backbone is responsible for a higher binding affinity. However, substitution of polyamide **5** with a γSN-turn induces a striking decrease of the binding affinity to all four base pairs relative to **4** and gives rise to a 8.7-fold increase in specificity for T•A in preference to A•T. The latter may stem from the same reasons as for the γSO-turn discriminating T•A pairs from the A•T pair and is clarified in Figure 3C,D with slow dissociation kinetics for binding to T•A, with a k_d of 2.7×10^{-2} s^{-1}, relative to A•T, with a k_d of 14×10^{-2} s^{-1} (Table 1). The dramatic reduction in affinity is possibly caused by at least three factors: (1) the relatively large protonated amino substituent has a steric clash with the floor of the DNA minor groove[18] and/or induces serious distortion of the minor groove, which is probably a predominant factor responsible for the weak binding affinity to G•C in the recognition event, (2) the hydrophobic environment in the interior of the DNA bases disfavors the electrostatic interaction of the polar amino group with any base, (3) such protonated amino groups have much weaker ability to form hydrogen bonds with acceptors of hydrogen bonding, such as the O2 of thymines and/or the N3 of guanines, than do *S*-hydroxyls. These results also suggest that the recognition properties of the polyamides with a hydroxyl/amino-modified γ-turn in the DNA minor groove are determined by a combination of factors, for example, hydrogen binding, compatibility, electrostatic interactions, environmental hydrophilicity/hydrophobicity, and so on.

Likewise, as shown in Supporting Information Table S1, the

Table 2. Preference for Recognition of Different γ-Turns to Four Base Pairs[a]

γ-turns	T·A	A·T	C·G	G·C
γ-turn	++	++	−	−
γRO-turn	++	+	−	−
γSO-turn	++	−	−	−
γRN-turn	++	+	−	−
γSN-turn	+	−	−	−

[a] Highly favored (++), favored (+), disfavored (−).

free energy change upon the formation of polyamide/DNA complexes can also quantitatively characterize the binding differences among these polyamides, especially with the demonstration in the energetics of a 1.2-fold increase in binding preference for T·A over A·T by γSN-turn. In short, the larger steric structure of the *S*-amino group directed at the floor of the DNA minor groove and the positive charge of the *R*-amino group oriented to the wall of the DNA minor groove may be dominant factors to control the separate binding events. On the basis of the above observations, we summarized the recognition code of the different functionalized γ-turns to the four base pairs, T·A, A·T, C·G, and G·C, at turn position in the DNA minor groove in Table 2.

Molecular Modeling Studies.

To get insight into the origin of the preferential binding of **3** to T·A over A·T, a plausible molecular model of the **3**-DNA complexes was estimated by energy minimization (Figure 4).[8a,11,19] As shown in Figure 4a, the hairpin polyamide **3** is significantly better docked in the DNA minor groove in an antiparallel manner into the sequence 5′-GCA**T**GCACATCG-3′/5′-CGATGTGC**A**TGC-3′, making close contact with the recognized T·A base pair by forming a hydrogen bond between the hydroxy group and the O2 of the T. In clear contrast, the γSO-turn of **3** in the complex of 5′-GCA**A**GCACATCG-3′/5′-CGATGTGC**T**TGC-3′ with an A·T base pair is lifted up from the minor groove (Figure 4b), and as can be seen in Figure 4d, the bulkier steric structure of the A base pushes the γ-monomer away from the floor of the minor groove to prevent the hydroxyl group from forming a strong hydrogen-bond interaction seen in the **3**-T·A complex. In the minimized structure, the distances between the α-hydroxy group of the γSO-turn and the O2 of the T or the N3 of the A are 1.87 and 3.28 Å in the recognition by **5** of sequences with T·A and A·T pairs, respectively (Figure 4c,d). In summary, the molecular modeling studies are in agreement with the SPR results and provide a molecular rationale for the thermodynamic observations.

Conclusion

Through the SPR technique, we found that the steric configuration of α-substituents in the γ-turns of four novel synthetic polyamides could lead to alteration of their binding properties to different DNA base pairs at the turn position relative to unmodified γ-turns. The polyamide with the γSO-turn favorably bound to T·A over A·T with a relatively high 25-fold increase in specificity, while the polyamide with the γSN-turn has a moderate selectivity of 8.7 in discriminating T·A from A·T. The molecular modeling studies suggest that the *S*-hydroxy-modified γ-aminobutyric acid acts as a T-recognition element in the DNA minor groove at the turn position. Deconvolution of degenerated T·A base pairs from A·T base pairs further increases the sequence specificity of the Py/Im polyamides.

Experimental Section

General Methods. The following abbreviations were used: DMF: *N*,*N*-dimethylformamide, DIEA: *N*,*N*-diisopropylethylamine, TFA: trifluoroacetic acid, HATU: *N*-{(dimethylamino)-1*H*-1,2,3-triazolo[4,5-b]-pyridino-1-ylmethylene}-*N*-methyl methan-aminium hexafluorophosphate, Boc: *t*-butoxycarbonyl, Fmoc: fluorenylmethoxycarbonyl, DMSO: dimethyl sulfoxide, β: β-alanine, γ or γ-turn: γ-aminobutyric acid, Hp: *N*-methyl-3-hydroxypyrrole, Py: *N*-methylpyrrole, Im: *N*-methylimidazole, Dp: 3-(dimethylamino)propylamine, Ac: acetyl, γSN: (*S*)-α,γ-diaminobutyric acid, γRN: (*R*)-α,γ-diaminobutyric acid, γSO: (*S*)-α-hydroxyl-γ-aminobutyric acid, γRO: (*R*)-α-hydroxyl-γ-aminobutyric acid, TIS: triisopropylsilane, DMS: dimethyl sulfide. ^{1}H NMR spectra were recorded on a JEOL JNM-FX400 superconducting NMR spectrometer at 400 MHz, with chemical shifts reported in parts per million relative to residual solvent and coupling constants in hertz. The following abbreviations were applied to spin multiplicity: s (singlet), d (doublet), t (triplet), q (quartet), qu (quintet), m (multiplet), dd (double doublet), and br (broad). Mass spectra were recorded on the following mass spectrometer using a positive ionization mode (unless otherwise stated): electrospray ionization mass spectrometry (ESI-mass) on an API 165 from PE SCIEX (Canada). Biacore assays were performed on a BIACORE X system (Sweden), and processing of data was carried out using BIAevalution version 4.1. High-performance liquid chromatography (HPLC) analysis was performed on Tosoh CCP & 8020 series using a ChemcoPak, Chemcobond, 5-ODS-H, 150 × 10 mm reversed-phase column in 0.1% AcOH in water with acetonitrile as eluent at a flow rate of 3.0 mL/min, a linear gradient elution of 0−100% acetonitrile in 30 min with detection at 254-nm detector (unless otherwise stated). Preparatory reversed-phase HPLC was performed on Tosoh CCP & 8020 series using a YMC-Pack R & D ODS, D-ODS-5-ST, S-5 μm, 150 × 20 mm reversed-phase column in 0.1% AcOH in water with acetonitrile as eluent at a flow rate of 6.0 mL/min, appropriate gradient elution conditions with detection at 254-nm or 350-nm detector. Collected fractions were analyzed by ESI-mass (PE SCIEX). All HPLC retention times quoted refer to the analytical column. Water (18 MΩ) was obtained from a Millipore MilliQ water purification system, and all buffers were 0.22-μm filtered and degassed in Biacore assays. HBS-EP buffer (0.01 M HEPES, pH 7.4, containing 0.15 M NaCl, 3 mM EDTA, and 0.005% Surfactant P20) and sensor chip SA were purchased from BIAcore AB (Sweden). Milligram quantities of polyamides were weighed on a precision microbalance and dissolved in 50 or 100 mL of HBS-EP buffer with 0.1% DMSO; second, an average molar extinction coefficient from three measurements at the absorption maximum of 295 nm was obtained on a UV spectrophotometer at 25 °C and used to determine the concentration of the polyamide solutions for **1**−**5** UV (HBS-EP buffer with 0.1% DMSO) λ_{max} (ϵ) 295 (49500). The molar extinction coefficients of the polyamides stayed constant, within ±10%, from 25 to 85 °C (Supporting Information Figure S1). Hairpin DNAs were obtained from Proligo and used without further purification. The biotinylated hairpin DNAs 5′-biotin-GGCCGATGTGC**N′**TGCTAT-AGCA**N**GCACATCGGCC-3′ (**N·N′**: T·A, A·T, C·G, and G·C) were obtained from Proligo. FmocImCOOH, FmocPyCOOH, DMF, DMSO, piperidine, and pyridine were from Wako (Osaka, Japan), and Fmoc-β-Ala-OH and Fmoc-γ-Abu-COOH were from Novabiochem. DIEA and *N*,*N*-dimethyl-1,3-propanediamine were from Nacalai Tesque, Inc. (Kyoto, Japan). TFA was from Kanto Chemical Co., Inc. (Tokyo, Japan). HATU was purchased from Peptide Institute, Inc. (Osaka, Japan). Clear resin (0.52 meq/g), (*R*)-α-*t*-butyloxycarbonylamino-γ-(9-fluorennylmethoxy)carbonylaminobutyric acid (**12**), and (*S*)-α-*t*-butyloxycarbonylamino-γ-(9-fluorennylmethoxy)carbonylaminobutyric acid (**13**) were available from Peptides International (Louisville,

(19) Bando, T.; Narita, A.; Sasaki, S.; Sugiyama, H. *J. Am. Chem. Soc.* **2005**, *127*, 13890−13895.

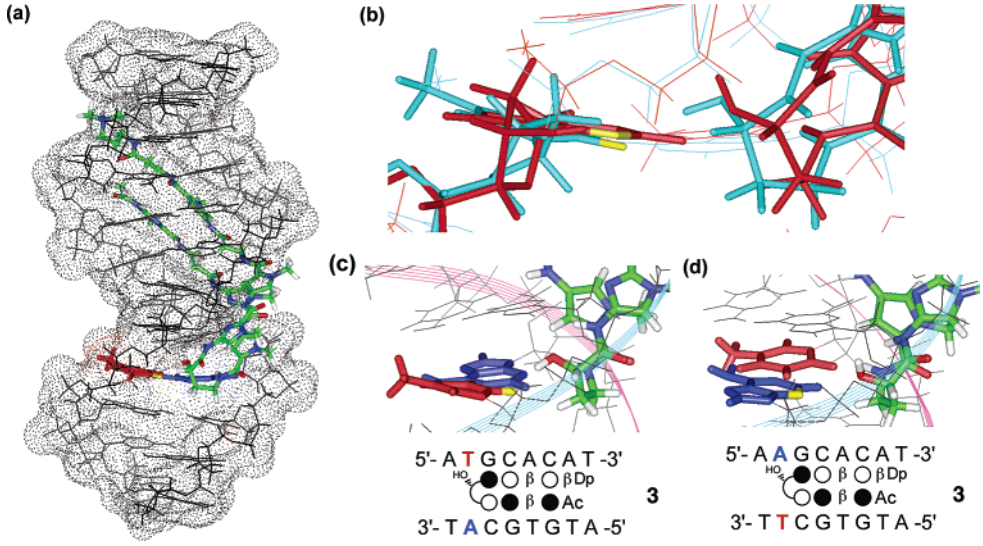

Figure 4. Molecular modeling study of the recognition by the polyamide with β/γSO of the sequence 5′-GCA**T**GCACATCG-3′/5′-CGATGTGC**A**TGC-3′. (a) A molecular model of the 1:1 complex of polyamide **3** with the sequence 5′-GCA(T/A)GCACATCG-3′/5′-CGATGTGC(A/T)TGC-3′ using a computer-assisted molecular simulation was obtained by energy miniziation. The polyamide is shown as a stick model, with the A base in blue and T base in red, but O2 in yellow, and in the polyamide, oxygen in red, hydrogen in gray, nirogen in blue, and carbon in green. (b) Superimposition of close-up of hairpin polyamide **3** with a γSO-turn and the sequence with an T·A base pair (cobalt blue) and A·T base pair (red). O2 of T and N3 of A is shown in yellow. (c) A close-up and schematic presentation of binding **3** with T·A base pair and (d) with A·T base pair.

KY). (2*R*)-2-*t*-Butyloxy-4-(9-fluorennylmethoxy)carbonylaminobutyric acid (**10**), (2*S*)-2-*t*-butyloxy-4-(9-fluorennylmethoxy)carbonylaminobutyric acid (**11**), and AcIm*β*ImPy-*γ*-ImPy*β*Py-*β*-Dp (**1**) were synthesized in the literature.[11] All other reagents and materials were from standard suppliers (highest quality available).

Polyamide Synthesis by Fmoc Chemistry. We used the same experimental conditions, methods, and instruments for synthesis of all polyamides **2**−**5** as those in the literature.[11] Data for **2**−**5** were the following:

AcIm*β*ImPy-*γ*RO-ImPy*β*Py-*β*-Dp (2). Yield: 8.53% as a white powder. Analytical HPLC: t_R = 11.60 min at a 98% minimum purity. ^{1}H NMR (400 MHz, DMSO-d_6): δ 10.35 (s, 1H, NH), 10.29 (s, 1H, NH), 10.18 (s, 1H, NH), 9.87 (s, 1H, NH), 9.83 (s, 1H, NH), 9.44 (s, 1H, NH), 8.04 (m, 1H, NH), 8.05 (m, 1H, NH), 7.98 (m, 1H, NH), 7.87 (t, J = 5.6 Hz, 1H, NH), 7.84 (t, J = 5.6 Hz, 1H, NH), 7.45 (s, 1H, aromatic CH), 7.43 (s, 1H, aromatic CH), 7.36 (s, 1H, aromatic CH), 7.20 (s, 2H, aromatic 2CH), 7.11 (d, J = 1.6 Hz, 1H, aromatic CH), 6.92 (m, 2H, aromatic 2CH), 6.62 (d, J = 1.6 Hz, 1H, aromatic CH), 4.14 (dd, J = 8.0 Hz, 3.6 Hz, 1H, CH_2CH_2CHOH), 3.95 (s, 3H, NCH_3), 3.94 (s, 3H, NCH_3), 3.90 (s, 3H, NCH_3), 3.80 (s, 3H, NCH_3), 3.79 (s, 3H, NCH_3), 3.76 (s, 3H, NCH_3), 3.51 (m, 2H, NHCH_2), 3.42 (m, 2H, NHCH_2), 3.32 (m, 4H, 2NHCH_2), 3.03 (q, J = 6.8 Hz, 2H, NHCH_2), 2.60 (t, J = 6.8 Hz, 2H, $COCH_2$), 2.46 (m, 2H, $N(CH_3)$-CH_2), 2.29 (t, J = 6.8 Hz, 2H, $COCH_2$), 2.15 (t, J = 7.2 Hz, 2H, COCH_2), 2.06 (s, 6H, $N(CH_3)_2$), 1.97 (s, 3H, $COCH_3$), 1.72 (m, 2H, CH_2CH_2CHOH), 1.48 (qu, J = 7.2 Hz, 2H, $CH_2CH_2CH_2$). ESI-mass: m/z calcd for $C_{53}H_{71}N_{21}O_{12}$: 1193.5591; found: 1194.5700 $[M + H]^+$, 597.7964 $[M + 2H]^{2+}$.

AcIm*β*ImPy-*γ*SO-ImPy*β*Py-*β*-Dp (3). Yield: 18.7% as a white powder. Analytical HPLC: t_R = 11.55 min at a 98% minimum purity. ^{1}H NMR (400 MHz, DMSO-d_6): δ 10.35 (s, 1H, NH), 10.29 (s, 1H, NH), 10.18 (s, 1H, NH), 9.89 (s, 1H, NH), 9.83 (s, 1H, NH), 9.42 (s, 1H, NH), 8.06 (m, 1H, NH), 8.00 (m, 1H, NH), 7.99 (m, 1H, NH), 7.90 (m, 1H, NH), 7.87 (m, 1H, NH), 7.45 (s, 1H, aromatic CH), 7.43 (s, 1H, aromatic CH), 7.36 (s, 1H, aromatic CH), 7.20 (s, 2H, aromatic 2CH), 7.11 (s, 1H, aromatic CH), 6.93 (d, J = 1.6 Hz, 2H, aromatic 2CH), 6.64 (s, 1H, aromatic CH), 4.14 (br, 1H, CH_2CH_2CHOH), 3.95 (s, 3H, NCH_3), 3.94 (s, 3H, NCH_3), 3.90 (s, 3H, NCH_3), 3.79 (s, 3H, NCH_3), 3.78 (s, 3H, NCH_3), 3.76 (s, 3H, NCH_3), 3.51 (m, 2H, NHCH_2), 3.41 (m, 2H, NHCH_2), 3.32 (m, 4H, 2NHCH_2), 3.05 (q, J = 6.8 Hz, 2H, NHCH_2), 2.59 (t, J = 5.6 Hz, 2H, $COCH_2$), 2.43 (m, 2H, $N(CH_3)$-CH_2), 2.31 (m, 4H, 2$COCH_2$), 2.28 (s, 6H, $N(CH_3)_2$), 1.97 (s, 3H, $COCH_3$), 1.74 (m, 2H, CH_2CH_2CHOH), 1.57 (m, 2H, $CH_2CH_2CH_2$). ESI-mass: m/z calcd for $C_{53}H_{71}N_{21}O_{12}$: 1193.5591; found: 1194.5987 $[M + H]^+$, 597.7986 $[M + 2H]^{2+}$.

AcIm*β*ImPy-*γ*RN-ImPy*β*Py-*β*-Dp (4). Yield: 20.5% as a white powder. Analytical HPLC: t_R = 9.95 min at a 98% minimum purity. ^{1}H NMR (400 MHz, DMSO-d_6): δ 10.35 (s, 1H, NH), 10.29 (s, 1H, NH), 10.07 (s, 1H, NH), 9.91 (s, 1H, NH), 9.85 (s, 1H, NH), 8.17 (m, 1H, NH), 8.07 (m, 1H, NH), 8.01 (m, 1H, NH), 7.96 (m, 1H, NH), 7.87 (m, 1H, NH), 7.47 (s, 1H, aromatic CH), 7.44 (s, 1H, aromatic CH), 7.36 (s, 1H, aromatic CH), 7.22 (s, 1H, aromatic CH), 7.21 (s, 1H, aromatic CH), 7.11 (d, J = 1.6 Hz, 1H, aromatic CH), 6.98 (s, 1H, aromatic 2CH), 6.93 (d, J = 1.6 Hz, 1H, aromatic CH), 6.64 (d, J = 1.6 Hz, 1H, aromatic CH), 3.95 (s, 3H, NCH_3), 3.94 (s, 3H, NCH_3), 3.90 (s, 3H, NCH_3), 3.80 (s, 6H, 2NCH_3), 3.76 (s, 3H, NCH_3), 3.51 (q, J = 6.4 Hz, 2H, NHCH_2), 3.41−3.32 (m, 7H, 4NHCH_2 and CH_2-CH_2CHNH_2), 3.07 (q, J = 6.4 Hz, 2H, NHCH_2), 2.60 (m, 4H, 2$COCH_2$), 2.47 (m, 2H, $N(CH_3)CH_2$), 2.43 (s, 6H, $N(CH_3)_2$), 2.31 (t, J = 6.8 Hz, 2H, $COCH_2$), 2.15 (t, J = 7.2 Hz, 2H, COCH_2), 1.97 (s, 3H, $COCH_3$), 1.80 (m, 2H, $CH_2CH_2CHNH_2$), 1.63 (qu, J = 7.2 Hz, 2H, $CH_2CH_2CH_2$). ESI-mass: m/z calcd for $C_{53}H_{72}N_{22}O_{11}$: 1192.5751; found: 1193.7769 $[M + H]^+$, 597.7783 $[M + 2H]^{2+}$.

AcIm*β*ImPy-*γ*SN-ImPy*β*Py-*β*-Dp (5). Yield: 9.80% as a light yellow powder. Analytical HPLC: t_R = 9.93 min at a 98% minimum purity. ^{1}H NMR (400 MHz, DMSO-d_6): δ 10.35 (s, 1H, NH), 10.29 (s, 1H, NH), 10.15 (s, 1H, NH), 9.90 (s, 1H, NH), 9.83 (s, 1H, NH), 8.06 (m, 2H, 2NH), 7.99 (m, 1H, NH), 7.87 (m, 1H, NH), 7.85 (m, 1H, NH), 7.44 (s, 1H, aromatic CH), 7.43 (s, 1H, aromatic CH), 7.36 (s, 1H, aromatic CH), 7.20 (s, 2H, aromatic 2CH), 7.11 (s, 1H, aromatic CH), 6.94 (m, 1H, aromatic CH), 6.93 (s, 1H, aromatic CH), 6.62 (s, 1H, aromatic CH), 3.94 (s, 6H, 2NCH_3), 3.90 (s, 3H, NCH_3), 3.79 (s, 6H, 2NCH_3), 3.76 (s, 3H, NCH_3), 3.51 (q, J = 6.4 Hz, 2H, NHCH_2), 3.41−3.32 (m, 7H, NHCH_2 and CH_2CH_2CHNH_2), 3.03 (q, J = 6.4 Hz, 2H, NHCH_2), 2.59 (m, 2H, $COCH_2$), 2.47 (m, 2H, $N(CH_3)CH_2$), 2.29 (t, J = 6.8 Hz, 2H, $COCH_2$), 2.19 (t, J = 6.8 Hz, 2H, COCH_2), 2.10 (s, 6H, $N(CH_3)_2$), 1.97 (s, 3H, $COCH_3$), 1.60 (m, 2H, CH_2CH_2-$CHNH_2$), 1.50 (qu, J = 7.2 Hz, 2H, $CH_2CH_2CH_2$). ESI-mass: m/z calcd for $C_{53}H_{72}N_{22}O_{11}$: 1192.5751; found: 1193.8657 $[M + H]^+$, 597.6786-$[M + 2H]^{2+}$.

Surface Plasmon Resonance Assay. All the SPR experiments were accomplished on a BIAcore X instrument at 25 °C according to the established protocol.[11] In short, after docked sensor chip SA into the instrument was handled through priming and preconditioning until the baseline was stable, denatured DNA was injected to flow over the chosen flow cell surface at a flow rate of 2 μL/min to obtain wanted immobilization level. Another unmodified flow cell was used as a reference. The polyamides were dissolved in DMSO to prepare ca. 10 μM stock solutions and stored at −30 °C. Before measurements, the stock solutions were diluted to 3.2 μM in HBS-EP buffer with 0.1% DMSO and the concentration was determined by UV absorption. The 3.2 μM solution was serially diluted twice to yield a concentration set of 1600, 800, 400, 200, 100, 50, 25, 12.5, 6.25, and 3.12 nM, and after normalization of immobilized sensor chip SA, sample solutions in HBS-EP buffer with 0.1% DMSO at different concentrations ranging from 3.12 nM to 1.6 μM were in turn injected at a flow rate of 5 μL/min in order of increasing concentration to minimize carryover using HBS-EP buffer with 0.1% DMSO as running buffer to obtain a series of sensorgrams. To obtain kinetics information, data processing was performed by global fitting of experimentally obtained sensorgrams to a model with mass transfer effects using the BIAevaluation 4.1 program.[16]

Molecular Modeling Studies. Molecular modeling was performed with the Insight II (2005) Discover (Accelrys, San Diego, CA) program, using CFF force field parameters. B-form DNA consisting of 5′-GCA**T**GCACATCG-3′/5′-CGATGTGC**A**TGC-3′ and 5′-GCA**A**GCA-CATCG-3′/5′-CGATGTGC**T**TGC-3′ was constructed by using the builder module of Insight II with standard B-form helical parameters (pitch, 3.38 Å; twist, 36; tilt, 1°). Polyamide **3** was built using the NMR structure of ImPyPy-γ-PyPyPy[8a] using standard bond lengths and angles. Docking was performed virtually by adjusting the DNA structure to permit minor groove binding according to the NMR structure of the ImPyPy-γ-PyPyPy-5′-d(CGCTAACAGGC)-3′/5′-d(GCCTGTTAGCG)-3′ complex.[8a] The assembled initial structure was energy-minimized with distance constraint of the putative hydrogen bonds, such as for the amido H and O2 of a pyrimidine or the N3 of a purine base, the N3 of imidazole and the $2NH_2$ of guanine, and the positively charged dimethylammonium H and O2 of C_{11}, and the 12 Watson−Crick base pairs. The minimization was done using a distance-dependent dielectric constant of $\epsilon = 4r$ (r stands for the distance between two atoms) and with convergence criteria having an RMS gradient of less than 0.001 kcal/mol Å. Eighteen Na cations were placed at the bifurcating position of the O−P−O angle at a distance of 2.51 Å from the phosphorus atom. The resulting complex was soaked in a 10 Å layer of water. The water was minimized first to the stage where the RMS was less than 0.001 kcal/mol Å, and then the whole system was minimized without any constraint under the same conditions.

Acknowledgment. We gratefully acknowledge the financial support from COE Project of Kyoto University Alliance for Chemistry. We also thank Dr. Bando for helpful discussions.

Supporting Information Available: BIAcore sensorgrams of polyamides **2** and **4** for recognition of 5′-**N**GCACA-3′ (**N** = T, A) and the standard free energy changes (ΔG°, kcal/mol) upon formation of polyamide/DNA complexes and molar extinction coefficient of polyamide **4** at different temperatures. This material is available free of charge via the Internet at http://pubs.acs.org.

JA064369L